Indication of a Universal Persistence Law Governing Atmospheric Variability

Eva Koscielny-Bunde,[1,2] Armin Bunde,[1] Shlomo Havlin,[1,2] H. Eduardo Roman,[1,3]
Yair Goldreich,[4] and Hans-Joachim Schellnhuber[5]
[1]*Institut für Theoretische Physik III, Universität Giessen, D-35392 Giessen, Germany*
[2]*Minerva Center and Department of Physics, Bar-Ilan University, Ramat Gan, 52900, Israel*
[3]*Dipartimento di Fisica and I.N.F.N., Università di Milano, I-20133 Milano, Italy*
[4]*Department of Meteorology, Bar-Ilan University, Ramat Gan, 52900, Israel*
[5]*Potsdam Institute for Climate Impact Research, D-14412 Potsdam, Germany*
(Received 14 January 1998)

We study the temporal correlations in the atmospheric variability by 14 meteorological stations around the globe, the variations of the daily maximum temperatures from their average values. We apply several methods that can systematically overcome possible nonstationarities in the data. We find that the persistence, characterized by the correlation $C(s)$ of temperature variations separated by s days, approximately decays $C(s) \sim s^{-\gamma}$, with roughly the same exponent $\gamma \cong 0.7$ for all stations considered. The range of this universal persistence law seems to exceed one decade, and is possibly even larger than the range of the temperature series considered. [S0031-9007(98)06602-2]

PACS numbers: 92.60.Wc, 02.70.Hm, 64.60.Ak, 92.60.Bh

The persistence of the weather is a well known phenomenon. If, for example, one day is sunny and warm, there is a high tendency that the next day remains similar. Persistence has been found also in successive years and is indicated by the finding of "red" noise in the power spectra of long-time meteorological records, but the specific law and the range of the persistence have not been clarified [1–3]. Here we study long-time daily temperature records (typically 100 years) obtained from 14 (randomly chosen) meteorological stations in Europe, North America, and Australia, from various climatological zones. To eliminate the (trivial) periodic seasonal trends, we analyzed the *variations* of the daily maximum temperatures from their average values. To eliminate further trends in the data, arising, e.g., as a result of urban warming, we applied, for the first time, detrended fluctuation analysis (DFA) [4] and wavelet techniques [5] that can systematically overcome possible nonstationarities in the data. Our analysis suggests that (i) the persistence, characterized by the correlation $C(s)$ of temperature variations separated by s days, follows a power law, $C(s) \sim s^{-\gamma}$, with roughly the same exponent $\gamma \cong 0.7$ for all stations considered, and that (ii) the range of this universal persistence law exceeds one decade. We cannot exclude the possibility that it even exceeds the range of the temperature series considered.

We have studied the records of the maximum daily temperatures T_i of the following weather stations (the length of the records is written within the parentheses): Albany (90 yr), Brookings (99 yr), Huron (55 yr), Luling (90 yr), Melbourne (136 yr), New York City (116 yr), Pendleton (57 yr), Prague (218 yr), Sidney (117 yr), Spokane (102 yr), Tucson (97 yr), Vancouver (93 yr), Moscow (115 yr), and St. Petersburg (111 yr). We are interested in the temperature fluctuations around their periodic seasonal trend. Therefore, we first determine the mean maximum daily temperature $\langle T_d \rangle$ for each calendar date d, say 1 May, by averaging over all years in the time series, and then we analyze the corresponding temperature deviations $\Delta T_i = T_i - \langle T_d \rangle$ from these mean values.

Qualitatively, persistence shows up already in plots of ΔT_i as shown in Fig. 1(a) for two successive years in Prague. The persistence is represented by relatively large patches of positive and negative ΔT_i. Indeed, when the data are randomly shuffled, the large patches disappear, as seen in Fig. 1(d). Quantitatively, persistence in the ΔT_i can be characterized by the (auto)correlation function,

$$C(s) \equiv \langle \Delta T_i \Delta T_{i+s} \rangle = \frac{1}{N - s} \sum_{i=1}^{N-s} \Delta T_i \Delta T_{i+s} \,. \quad (1)$$

If there is no persistence, the ΔT_i are uncorrelated and $C(s)$ is zero for s positive. If persistence exists up to a certain number of days s_p, the correlation function will be positive up to s_p and vanish above s_p. A direct calculation of $C(s)$ is hindered by the level of noise present in the finite temperature series, and by possible nonstationarities in the data (see, e.g., [6]). To reduce the noise we do not calculate $C(s)$ directly, but instead study the temperature "profile" [Fig. 1(b)]

$$Y_n = \sum_{i=1}^{n} \Delta T_i \,. \quad (2)$$

We can consider the profile Y_n as the position of a random walker on a linear chain after n steps. The random walker starts at the origin of the chain and performs, in the ith step, a jump of length ΔT_i to the right, if ΔT_i is positive, and to the left, if ΔT_i is negative. According to random walk theory (see, e.g., [7]), the fluctuations (standard deviation, see below) $F(s)$ of the profile in a given "time window" of length s are related to the correlation

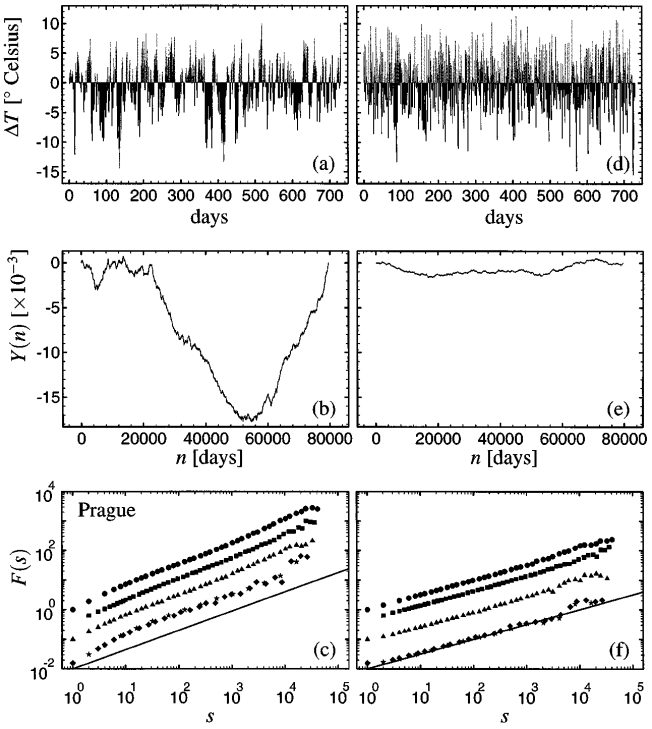

FIG. 1. (a) Daily temperature variations $\Delta T_i = T_i - \langle T_d \rangle$ from 1 January 1900 until 31 December 1901 in Prague. (b) The temperature profile $Y_n = \sum_{i=1}^{n} \Delta T_i$ for Prague, for the entire 218 yr (1775–1992). (c) The fluctuation function $F(s)$ obtained (i) from the standard fluctuation analysis (FA) (circles), (ii) from the detrended fluctuation analysis (DFA) (squares), (iii) from the first derivative wavelet method (WL1) (triangles), and (iv) from the second (diamonds) and third (stars) derivative wavelet method (WL2, WL3). In the log-log plot, the curves obtained by the detrended methods (DFA, WL2, and WL3) appear to be approximate straight lines for s above 10 days, and their slope $\alpha \cong 0.65$ (shown as straight line in the figure) is related to the correlation exponent γ by $\gamma = 2 - 2\alpha$, yielding $\gamma \cong 0.7$. (d)–(f) The analog curves to (a)–(c), respectively, when the ΔT_i are randomly shuffled. In this case, due to the shuffling, the correlations have been removed, and the fluctuation function $F(s)$ is proportional to $s^{1/2}$, as indicated by the straight line with slope 1/2 in (f).

function $C(s)$. For the relevant case of long-range power-law correlations

$$C(s) \sim s^{-\gamma}, \qquad 0 < \gamma < 1, \tag{3}$$

the fluctuations $F(s)$ increase by a power law [7],

$$F(s) \sim s^{\alpha}, \qquad \alpha = 1 - \gamma/2. \tag{4}$$

For uncorrelated data [as well as for short-range correlations represented by exponentials $C(s) \propto \exp(-s/s_p)$ or $\gamma \geq 1$], we have $\alpha = 1/2$.

To find how the fluctuations scale with s, we divide the profile into nonoverlapping segments of size s. We calculate the square fluctuations $F_\nu^2(s)$ in each segment ν and obtain $F(s)$ by averaging over all segments, $F(s) \equiv \langle F_\nu^2(s) \rangle^{1/2}$ [8]. We employed four methods that differ in the way the fluctuations are measured and possible nonstationarities are eliminated:

(i) In the (standard) fluctuation analysis (FA), we consider the profile at both ends of each segment ν, $Y_{(\nu+1)s}$ and $Y_{\nu s}$, and identify the square of the fluctuations in this segment as $F_\nu^2(s) = (Y_{(\nu+1)s} - Y_{\nu s})^2$.

(ii) In the "detrended" fluctuation analysis, we determine in each segment the best linear fit of the profile, and calculate the standard deviation of the profile from this straight line. This way, we eliminate the influence of possible linear trends on scales larger than the segment [4].

More advanced techniques are wavelet methods [5], which are based on the determination of the mean values $\overline{Y}_\nu(s)$ of the profile in each segment ν and the calculation of the fluctuations between neighboring segments.

(iii) In the first-order wavelet method (WL1), we determine $F_\nu^2(s) = [\overline{Y}_\nu(s) - \overline{Y}_{\nu+1}(s)]^2$.

(iv) In the higher-order wavelet methods (WL2 and WL3), we determine $F_\nu^2(s) = [\overline{Y}_\nu(s) - 2\overline{Y}_{\nu+1}(s) + \overline{Y}_{\nu+2}(s)]^2$ and $F_\nu^2(s) = [\overline{Y}_\nu(s) - 3\overline{Y}_{\nu+1}(s) + 3\overline{Y}_{\nu+2}(s) - \overline{Y}_{\nu+3}(s)]^2$.

Methods (iii) and (iv) are called wavelet methods, since they can be interpreted as transforming the profile by square wavelets representing first-, second-, and third-order cumulative derivatives of the profile.

By construction, FA and WL1 are sensitive to linear trends, while DFA and WL2 can eliminate them. WL3 can, in addition, eliminate also parabolic types of trends. These methods are superior to the conventional power spectra methods (see, e.g., [9]), where Fourier transforms $S(f)$ of annual temperature correlations are considered. A typical power spectrum consists of various oscillatory maxima and nonconstant background noise ("red noise"), which arises from (correlated) temperature fluctuations. Power-law correlations [see Eq. (3)] will lead to a corresponding power-law decay of $S(f), S(f) \sim f^{-(1-\gamma)}$, which is, however, in our case hidden by the additional oscillatory maxima and therefore cannot be detected unambiguously. The methods we use here are more efficient for detecting long-term persistence laws, do not involve fit parameters, and have already been applied successfully to biological sequences (heart beat intervals and DNA sequences [4,5]) where nonstationarities are known to occur.

We begin the analysis with the temperature series $\{\Delta T_i\}$ for Prague which is the longest series (218 yr) in this study. Figure 1(b) shows the profile, and Fig. 1(c) shows the fluctuation functions $F(s)$ obtained from the four methods. In the log-log plot, all curves are approximately straight lines for s above 10 days, with a slope $\alpha \cong 0.65$. This result suggests that there exists long-range persistence expressed by the power-law decay of the correlation function with an exponent $\gamma \cong 0.7$. A closer look at the curves in Fig. 1(c) indicates that the effects of trends and correlations can, to a certain extent, be distinguished by the methods. At about 10^3 days, the curves of FA and WL1 show a slight crossover toward a larger exponent α. This behavior can be interpreted as the effect of the warming of Prague due to urban

development. In contrast, DFA, WL2, and WL3 yield approximate straight lines until about 10^4 days above which the data start to scatter. The systematic crossover at about 10^3 days does not occur here, since DFA, WL2, and WL3 eliminate the (roughly) linear trend of warming.

To test our claim that the slope $\alpha \cong 0.65$ is due to long-range correlations, we have eliminated the correlations by randomly shuffling the ΔT_i. This shuffling has no effect on the probability distribution function of the ΔT_i, which we found to be approximately Gaussian. Figures 1(d)–1(f) show the effect of shuffling on (d) the daily temperature fluctuations ΔT_i, (e) the profile, and (f) the fluctuation functions. By comparing Figs. 1(a)–1(c) with 1(d)–1(f), we see the effect of correlations: The uncorrelated ΔT_i are less patchy, the uncorrelated profile shows much smaller deviations from the (fixed) values at the end points, and the exponent α characterizing the fluctuations in the shuffled uncorrelated sequence is $1/2$, as expected. For a further confirmation of our findings, we have also tested $F(s)$ for short-range correlations by dividing the temperature record into segments of 50 days and shuffling the segments. We obtained that $F(s)$ crosses over to $s^{1/2}$ above $s \cong 50$, in agreement with the expectation.

Further representative examples are shown in Figs. 2(a)–2(e), where we plotted the fluctuation functions for New York City (116 yr), Luling from Texas (90 yr), Spokane from Washington State (102 yr), Melbourne (136 yr), and Sydney (117 yr). The straight lines shown in the double-logarithmic plots have slope 0.65. Similar to Prague, the effect of local warming is also seen in New York and Sydney. For Spokane, the FA and WL1 curves also seem to exhibit a slight crossover, while for Luling and Melbourne the curves are straight lines without any crossover. Our main point is that the detrended methods (DFA, WL2, and WL3) yield, for all stations considered, approximate straight lines with roughly the same slope around 0.65. Because of lack of statistics, the data scatter strongly for large s (above 10 yr), and the actual range of the correlations cannot be detected.

To test the methods further and to see which range of correlation can be detected from the data, we have also analyzed artificial sequences of similar length as the sequences in (a)–(e), with the correlation exponent 0.65. A representative result is shown in Fig. 2(f). Apart from very small s values, the artificial curves look similar as the realistic detrended ones. Above an s value that is about 10% of the length N of the artificial series, the data start to scatter and the true range of correlations cannot be detected. Hence, from our analysis of the real data we cannot exclude the possibility that the time range of the persistence law found here may even exceed the length of the presently available temperature series.

Our finding of long-range power-law persistence with roughly the same exponent α for different weather stations in different climatic zones and in different time regimes (self-similarity from weeks to decades of years) suggests that atmospheric variability is governed by rather fundamental mechanisms, leading to temperature fluctuations *similar* in different places and on different time scales. The extremely long persistence of the fluctuations suggests that the coupling of atmospheric and oceanic processes has to be involved, as the latter rule the long-term dynamics of the system. The importance of this coupling has been emphasized in the context of interdecadal and century-scale climate oscillations [10], and is currently one of the core questions in climatology [11].

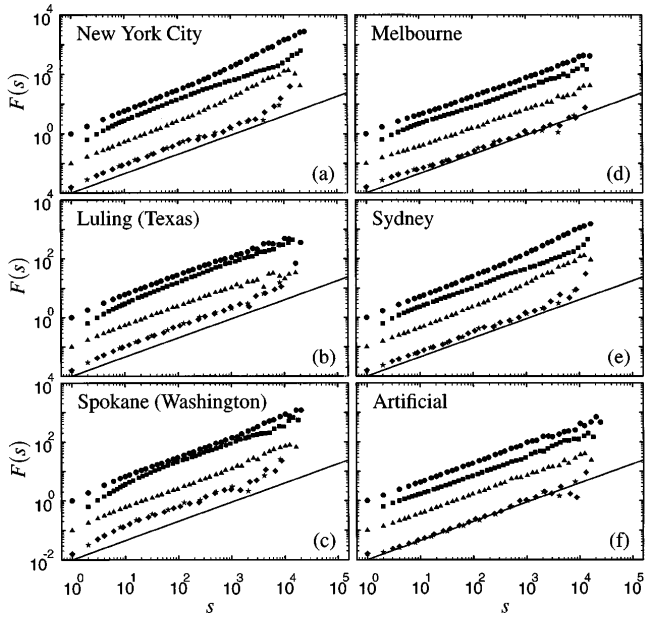

FIG. 2. The fluctuation functions $F(s)$ versus s obtained from FA, DFA, WL1, WL2, and WL3, in a double logarithmic plot, for five representative weather stations (a)–(e) and (f) one sequence of 40 000 artificial random data with a correlation exponent $\gamma = 0.7$. For the different analysis methods, we used the same symbols as in Figs. 1(c), 1(f). For $s > 10$, the curves obtained by the detrended methods (DFA, WL2, and WL3) appear to be approximate straight lines, with slopes around $\alpha \cong 0.65$ (shown as straight lines in the figures), yielding the correlation exponent $\gamma \cong 0.7$.

Moreover, our findings may be relevant to the current debate over anthropogenic global warming [12]. While most climatologists hold that there is already empirical evidence for human interference with the climate, a few others strongly disagree [13]. Given the operable bulk of meteorological observations, the crucial point is to distinguish the "authropogenic signal" from the "noise" generated by the natural variability of the geophysical system. Climatologists try to circumvent this problem, e.g., by complementing empirical data with simulated ones obtained from coupled ocean-atmosphere circulation models (see, e.g., [14]). The results of the various models are partially conflicting (see, e.g., [15]), and we believe that the universal power-law relation we found can serve as a very useful test [16] for the competing climate models and of the basic assumptions underlying them.

We are grateful to W. Gerstengarbe and P. C. Werner for providing us with the temperature records, and thank

G.I.F. for financial support. We are very much indebted to K. Fraedrich for helpful discussions.

[1] O. M. Essenwanger, in *World Survey of Climatology*, edited by H. E. Landsberg (Elsevier, Amsterdam, 1986), Vol. 1B; S. B. Newman, Weather Forecasting **6**, 111 (1991).

[2] J. E. Kutzbach and R. A. Bryson, J. Atmos. Sci. **31**, 1958 (1974); K. Hasselmann, Tellus **28**, 473 (1975); E. B. Kraus, Mon. Weather Rev. **105**, 1009 (1977).

[3] For more recent studies, see M. R. Allen and L. A. Smith, Geophys. Res. Lett. **21**, 883 (1994); M. E. Mann and J. M. Lees, Clim. Change **33**, 409 (1996); Ref. [15] of this paper, and further references quoted in these articles.

[4] C. K. Peng *et al.*, Phys. Rev. E **49**, 1685 (1994); S. V. Buldyrev *et al.*, Phys. Rev. E **51**, 5084 (1995).

[5] A. Arneodo *et al.*, Phys. Rev. Lett. **74**, 3293 (1995); A. Arneodo *et al.*, Physica (Amsterdam) **96D**, 291 (1996); for a general review on wavelets, see, e.g., M. Vetterli and J. Kovacevic, *Wavelets and Subbane Coding* (Prentice-Hall, Englewood Cliffs, NJ, 1995).

[6] C. D. Schönwiese and J. Rapp, *Climate Trend Atlas of Europe Based on Observations 1891–1990* (Kluwer, Dordrecht, 1997).

[7] A.-L. Barabasi and H. E. Stanley, *Fractal Concepts in Surface Growth* (Cambridge University Press, 1995); M. F. Shlesinger, B. J. West, and J. Klafter, Phys. Rev. Lett. **58**, 1100 (1987).

[8] In addition to the average $F(s) \equiv \langle F_\nu^2(s)\rangle^{1/2}$ discussed above, we have also studied the more general average $F_q(s) \equiv \langle F_\nu^q(s)\rangle^{1/q}$, $q > 0$. We have found that $F_q(s)$ was independent of q and therefore can be identified with $F(s)$. A discussion of these general moments and the scaling behavior of the corresponding probability distribution function will be published elsewhere.

[9] G. E. P. Box, G. M. Jenkins, and G. C. Reinsel, *Time Series Analysis* (Prentice-Hall, Englewood Cliffs, NJ, 1994), 3rd ed.; M. R. Allen and L. A. Smith, J. Clim. **9**, 3373 (1996).

[10] M. E. Mann, J. Park, and R. S. Bradley, Nature (London) **378**, 266 (1995); P. Chang, L. Ji, and H. Li, Nature (London) **385**, 516 (1997); R. T. Sutton and M. R. Allen, Nature (London) **388**, 563 (1997).

[11] World Climate Research Programme, Newsletter No. 1, Geneva, 1996.

[12] *Climate Change 1995: The Science of Climate Change*, edited by J. T. Houghton *et al.* (Cambridge University Press, Cambridge, England, 1996).

[13] K. Hasselmann, Science **276**, 914 (1997).

[14] G. C. Hegerl, H. v. Storch, K. Hasselmann, B. D. Santer, U. Cubasch, and P. D. Jones, J. Clim. **9**, 2281 (1996).

[15] T. Barnett *et al.*, Holocene **6**, 255 (1996).

[16] For a very preliminary test of two state-of-the-art climate models, we analyzed Fig. 1 in Ref. [15] where power spectra of model annual temperature series (GFDL and MPI Hamburg, respectively) have been compared. We found that one of the model outputs (GFDL) is consistent with our result, while the other one (MPI Hamburg) is not.